Electronic Supplementary Information

A bipolar pyridine functionalized porphyrin with hybrid charge-storage for dual-ion batteries

Fangfang He,[a] Yangmei Zhou [a], Xi Chen [a], Ting Wang [a], Youlian Zeng [a], Jiahao Zhang [a], Zhi Chen[b,] *, Wei Liu[c] and Ping Gao [a,]*

[a.] *Key Laboratory of Environmentally Friendly Chemistry and Applications of Ministry of Education, College of Chemistry, Xiangtan University, Xiangtan 411105, China. Email: ping.gao@xtu.edu.cn*

[b.] *College of Chemistry and Environmental Engineering, Shenzhen University, Shenzhen 518071, China. Email: Zhi.Chen@szu.edu.cn*

[c.] *Yiyang Hongyuan Rare Earth Co., Ltd, Yiyang 413001, P. R. China*

Experimental section

1.1 *Materials:*

All reactants and solvents were obtained from Alfa Aesar and Chemical Greatwall. Polyvinylidene fluoride (PVDF), acetylene black, and N-methyl-2-pyrrolidone (NMP), Glass microfiber filters (Whatman, GF/D), stainless steel (316L, 12 mm in diameter) were purchased commercially and used as received without further purification. Compound (5,10,15,20-tetra(4-pyridinyyl)-21H,23H-porphyrin) (T4PP) was received from Shanghai Tensus Biotech CO.,Ltd.

1.2 *Structural characterization:*

UV-Vis spectra of porphyrins were measured on a Perkin–Elmer Cary 60 spectrometer. Mass spectrometry (MS) data were performed on a Bruker Aupoflflex III MALDI-TOF Analyzer using CCA as matrix. The morphology of samples was carried out using field emission scanning electron microscope (SEM, JSM-6610LV). The attenuated total reflectance-Fourier transformation infrared (ATR-FTIR) spectroscopy was obtained on a Thermo Fisher Nicolet IS50 ATR-FTIR spectrometer from 520 cm^{-1} to 4000 cm^{-1}. Power X-ray diffraction patterns (XRD) were recorded using a D8 ADVANCE X-ray diffractometer with a Cu Ka radiation source (λ = 0.154 nm). X-ray photoelectron Spectroscopy was recorded on a Escalab250Xi (Thermo Scientific), using monochromatized Al Kα radiation (1486 eV). The pass energy for survey spectra was 100 eV, for detail spectra the energy was 30 eV. The binding energies of all spectra were calibrated with respect to the C1s peak of ubiquitous carbon at a binding energy of 284.8 eV.

1.3 *Electrochemical measurements:*

The T4PP and CuT4PP electrode were prepared by mixing 40 wt % acetylene black,

10 wt % PVDF and 50 wt % T4PP (or CuT4PP) and the slurry was coated onto stainless

steel current collectors (12 mm in diameter). The T4PP and CuT4PP electrode were coupling with alkali metal (Li, Na) foils, while 1 M lithium hexafluorophosphate ($LiPF_6$) in ethylene carbonate (EC): dimethyl carbonate (DMC): propylene carbonate (PC)

(1:3:1 by volume ratio) or 1 M sodium hexafluorophosphate ($NaPF_6$) in propylene carbonate (PC) were used as electrolyte. The mass loading of active material was around 1.5 mg cm^{-2}. All capacities were calculated based on active material of electrode. Cyclic voltammetry (CV) and Electrochemical impedance spectroscopy (EIS) were conducted on an electrochemical workstation (CHI600E). Galvanostatic charge/discharge measurements were performed with a Neware battery testing system at 298 K. CR-2032 coin cells were assembled in an argon-filled glove box (MIKROUNA) with oxygen and water concentration lower than 0.1 ppm.

The electrodes of ex-situ studies (including XPS, IR, Raman and XRD) were prepared by mixing 10 wt % acetylene black, 10 wt % PVDF and 80 wt % T4PP and the slurry was coated onto stainless steel current collectors (12 mm in diameter). Then the electrodes were assembled with lithium metal foils into cells. The cells were disassembled after charged/discharged to specific state of charge, and the electrodes were rinsed several times by the solvent (DME) and dried in an argon-filled glove box for characterization.

1.4 Synthesis of [5,10,15,20-tetra(4-pyridinyl)-porphinato] copper (II) (CuT4PP)

Compound (5,10,15,20-tetra(4-pyridinyyl)-21H,23H-porphyrin) (T4PP) (123.6 mg, 0.2 mmol) and $Cu(OAc)_2 \cdot H_2O$ (99.825 mg, 0.5 mmol) were dissolved in a mixed solvent of dimethylformamide (DMF) and AcOH (1:1, v:v). The reaction suspension was stirred under 150℃ overnight, giving a homogeneous solution. The solution was cooled to room temperature to precipitate a dark purple crystalline solid. The solid was collected by filtration, washed with water, and dried at 150 °C under vacuum to give CuT4PP (105.4mg, 85% yield). UV-Vis ($CHCl_3$, nm) 415,538. MALDI-TOF calc. for C40H24N8Cu: $[M]^+$, 679.14; Found: m/z 679.02.

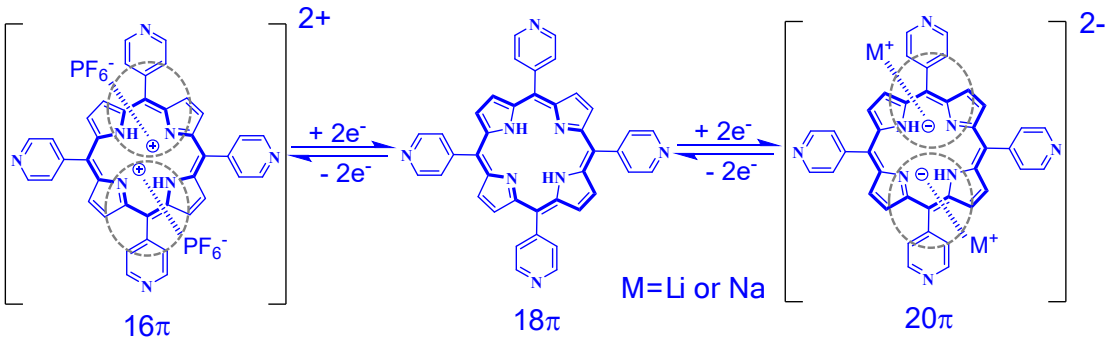

Scheme S1. The proposed reaction mechanism of the T4PP in Li/Na batteries.

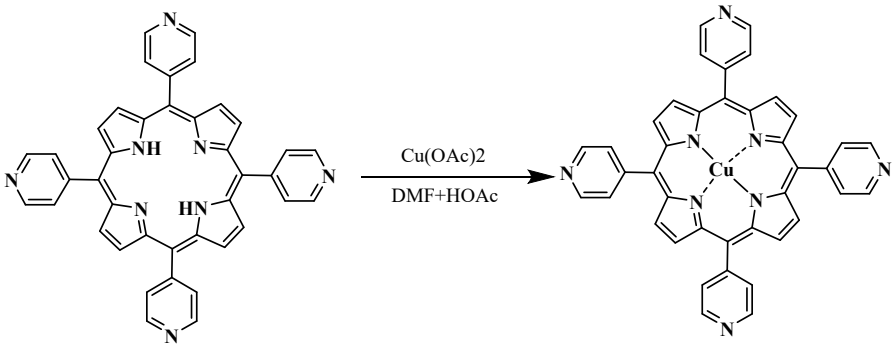

Scheme S2. Synthetic procedures of **CuT4PP**.

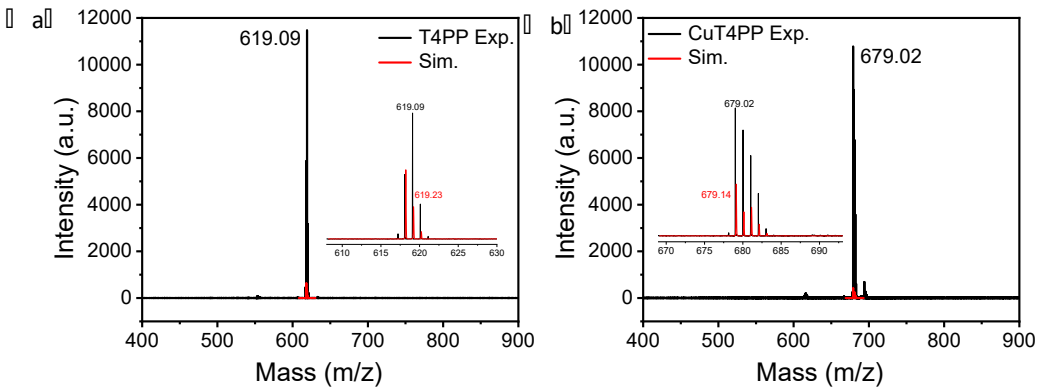

Fig. S1. MALDI-TOF mass spectrum of the T4PP (a) and CuT4PP (b).

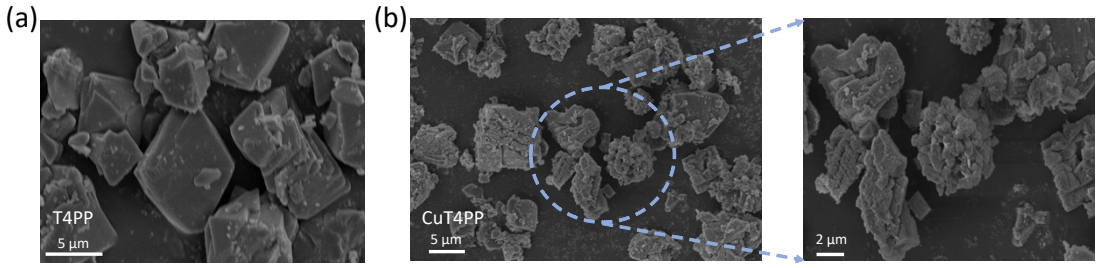

Fig. S2. SEM images of (a) T4PP and (b) CuT4PP.

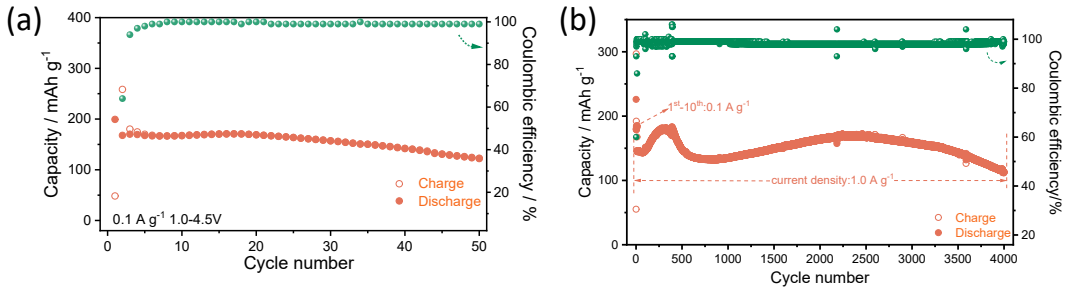

Fig. S3. (a) Cycling performance of T4PP for LDIBs at 0.1 A g^{-1}, (b) long-term cycling performance of T4PP at 1.0 A g^{-1} in a voltage range of 4.5-1.0 V (vs. Li^+/Li).

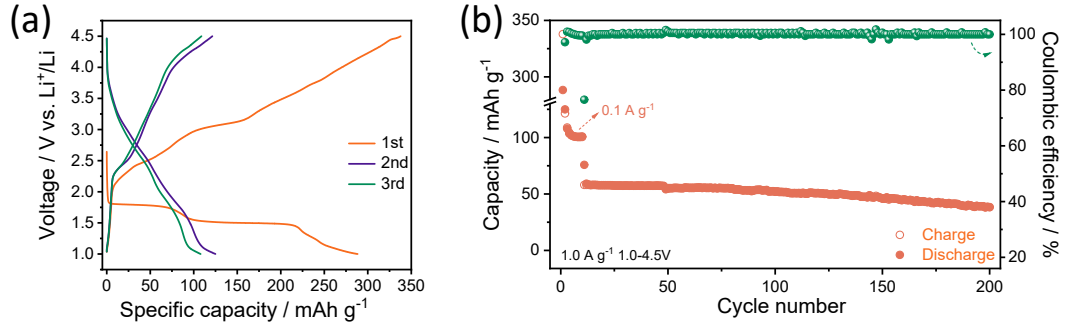

Fig. S4. (a) Initial discharge-charge curves and (b) long-term cycling performance of T4PP at 1.0 A g^{-1} in a voltage range of 4.5-1.0 V (vs. Li^+/Li).

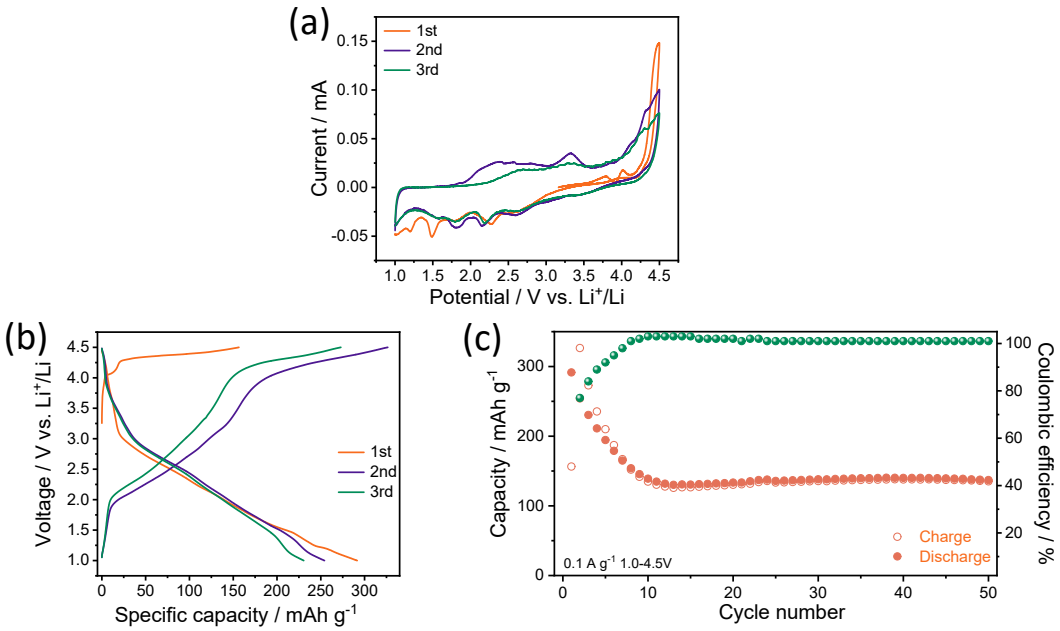

Fig. S5. (a) CV curves of CuT4PP at a sweep rate of 0.1 mV s^{-1}, (b) galvanostatic charge and discharge profile and (c) cycling performance at 0.1 A g^{-1} in the range of 4.5-1.0 V (vs. Li^+/Li).

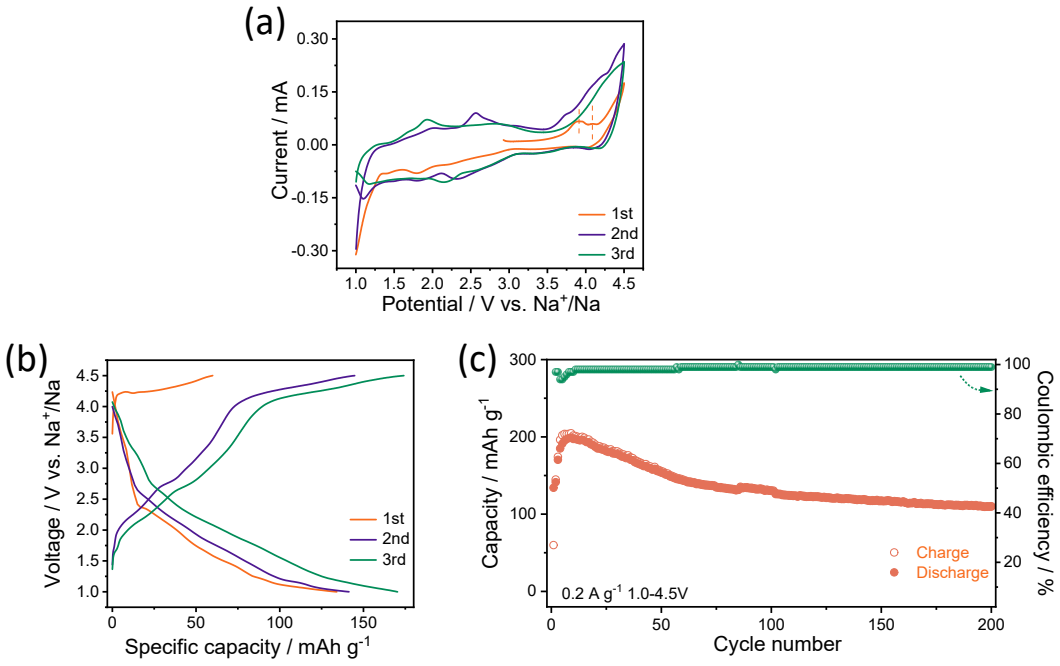

Fig. S6. (a) CV curves of CuT4PP at a scan rate of 0.5 mV s^{-1}, (b) galvanostatic charge and discharge curves and (c) cycling performance at 0.2 A g^{-1} in the range of 4.5-1.0 V (vs. Na^+/Na).

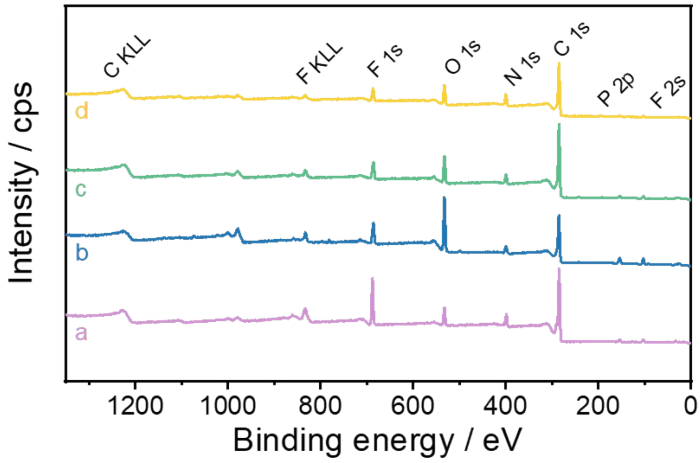

Fig. S7. Survey XP spectra of T4PP at a, b, c, and d states. (a-d denote as-prepared, charged, discharged, recharged T4PP).

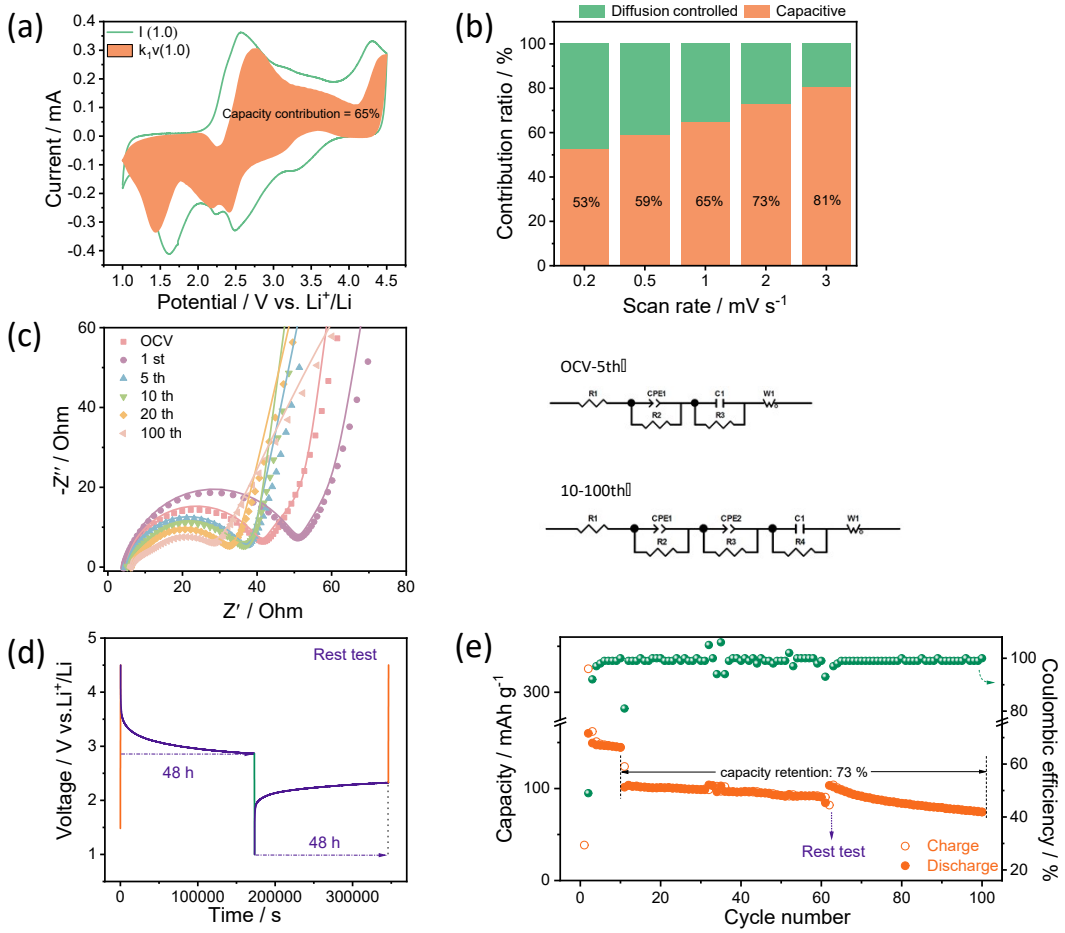

Fig. S8. (a) capacitive contributions (shaded area) to charge storage at a scan rate of 1 mV s^{-1}, (b) contribution ratio of the pseudocapacitance at various scan rates, (c) EIS and equivalent circuit model of T4PP electrode, (d) voltage evolution over time, (e)

capacity evolution of T4PP (The Li/$LiPF_6$/T4PP cell was activated 10 times at 0.1 A g^{-1}, and continued to run 50 cycles at 1 A g^{-1} to achieve a stable cycle, the 61st circle was fully charged to 4.5 V and then rested for 48 h, and then discharged completely to 1.0 V and continued to rest for 48 h. Finally, the battery proceeded.)